

Structure and Dynamics of the 1-Hydroxyethyl-4-amino-1,2,4-triazolium Nitrate High-Energy Ionic Liquid System

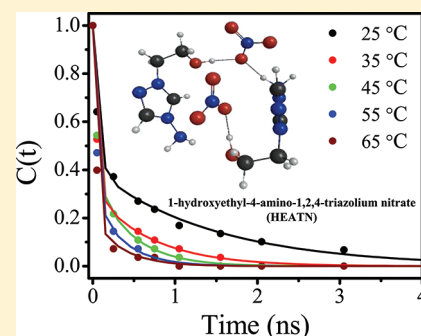
Philip J. Carlson,[†] Sayantan Bose,[†] Daniel W. Armstrong,[‡] Tommy Hawkins,[§] Mark S. Gordon,^{*,†} and Jacob W. Petrich^{*,†}

[†]U.S. Department of Energy Ames Laboratory and Department of Chemistry, Iowa State University, Ames, Iowa 50011, United States

[‡]Department of Chemistry and Biochemistry, University of Texas, Arlington, Box 19065, Arlington, Texas 76019, United States

[§]Air Force Research Laboratory, 10 East Saturn Boulevard, Building 8451, Edwards Air Force Base, California 93524, United States

ABSTRACT: An investigation of the structure and dynamics of the high-energy ionic liquid, 1-hydroxyethyl-4-amino-1,2,4-triazolium nitrate (HEATN), was undertaken. Both experimental and computational methods were employed to understand the fundamental properties, characteristics, and behavior of HEATN. The charge separation, according to the electrostatic potential derived charges, was assessed. The MP2 (second-order perturbation theory) geometry optimizations find six dimer and five tetramer structures and allow one to see the significant highly hydrogen bonded network predicted within the HEATN system. Due to the prohibitive scaling of ab initio methods, the fragment molecular orbital (FMO) method was employed and assessed for feasibility with highly energetic ionic liquids using HEATN as a model system. The FMO method was found to adequately treat the HEATN ionic liquid system as evidenced by the small relative error obtained. The experimental studies involved the investigation of the solvation dynamics of the HEATN system via the coumarin 153 (C153) probe at five different temperatures. The rotational dynamics through the HEATN liquid were also measured using C153. Comparisons with previously studied imidazolium and phosphonium ionic liquids show surprising similarity. To the authors' knowledge, this is the first experimental study of solvation dynamics in a triazolium-based ionic liquid.



INTRODUCTION

There has been a steeper than exponential growth in the number of publications related to ionic liquids since the year 2000.¹ The interest in ionic liquids reflects their versatility and their environmentally friendly properties in comparison to commonly used compounds.^{2–4} Ionic liquids are molten salts, commonly composed of an organic cation and an inorganic anion that can often be liquid at room temperature. These low-melting salts are considered to be green solvents, in contrast to volatile organic compounds, due to their high chemical and thermal stabilities, negligible vapor pressure,⁵ and high recoverability and reusability.^{6,7} Ionic liquids can be customized by varying the identity of the substituents on the cation or by adapting the moiety of the anion.⁸ This versatility and these unique properties have piqued the interest of the scientific community, and a variety of fundamental studies^{9–16} have been performed on ionic liquids to obtain a better understanding of their characteristics.

One interesting application of ionic liquids is in the high-energy density matter (HEDM) community, where many different molten salts have been explored and reported.¹⁷ It is important to understand what characteristics make ionic liquids suited to HEDM applications. This very problem was explored computationally in a series of studies,^{18–20} as well as experimentally in a few reports.²¹ These studies show that triazolium ionic liquids appear to have more suitable characteristics for HEDM applications than other nitrogen-rich ionic liquid species.

A recent report by Drake and co-workers²² on low-melting, potentially energetic salts lists their desired characteristics, as well as potential benefits, that might be derived from using them in energetic materials applications. The same authors have discussed the 1-R-4-amino-1,2,4-triazolium family of salts²³ that are of interest owing to their high nitrogen content. One interesting room-temperature ionic liquid in this family is 1-hydroxyethyl-4-amino-1,2,4-triazolium nitrate (HEATN), depicted in Figure 1a. To use the HEATN ionic liquid in various applications, it is beneficial to employ both experimental and computational methods to understand the fundamental properties, characteristics, and behavior of HEATN.

This present work focuses on the physical chemistry of the high-energy ionic liquid system HEATN. The HEATN system was recently investigated using molecular dynamics simulations for the prediction of bulk properties.²⁴ The studies presented here assess this ionic liquid at a molecular level, using ab initio electronic structure methods, to gain insight into the structure, energetics, and charge delocalization in the component ions. These properties have been shown to be of significance in relation to the physical and chemical properties of ionic liquids,²⁵ and ab initio electronic structure methods have provided

Received: August 15, 2011

Revised: October 31, 2011

Published: November 29, 2011

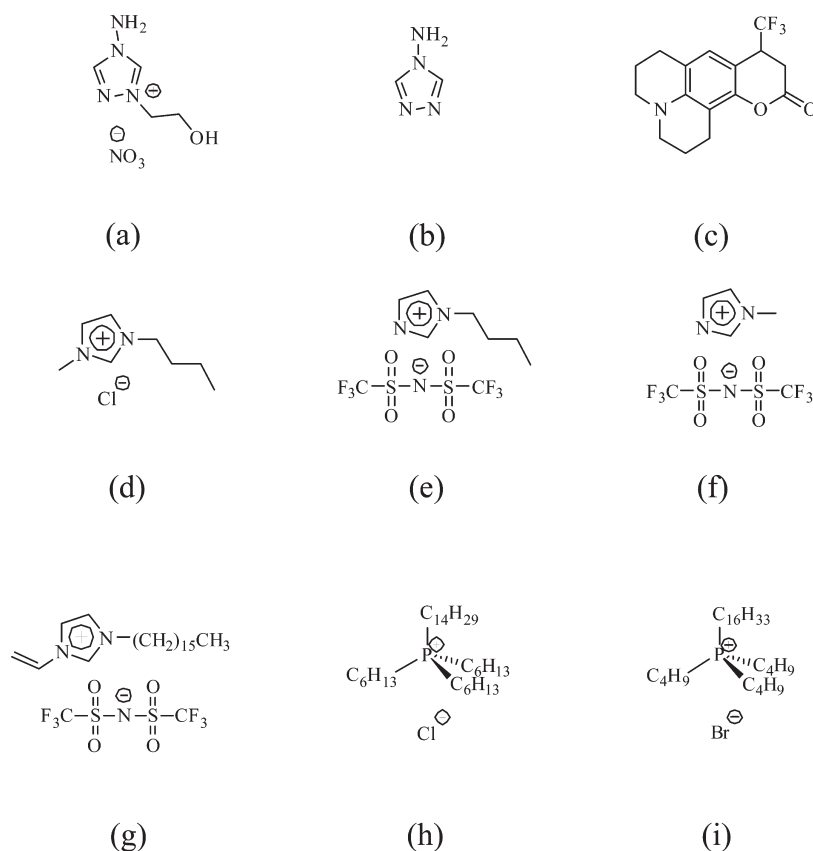


Figure 1. Structures of (a) 1-hydroxyethyl-4-amino-1,2,4-triazolium nitrate (HEATN), (b) 4-amino-1,2,4-triazole, (c) solvatochromic probe coumarin 153 (C153), (d) 1-butyl-3-methylimidazolium chloride (BMIM⁺ Cl[−]), (e) 1-butylimidazolium bis(trifluoromethylsulfonyl)imide (BIM⁺ NTf₂[−]), (f) 1-methylimidazolium bis(trifluoromethylsulfonyl)imide (MIM⁺ NTf₂[−]), (g) 1-cetyl-3-vinylimidazolium bis(trifluoromethylsulfonyl)imide (CVIM⁺ NTf₂[−]), (h) tetradecyl trihexyl phosphonium chloride, and (i) hexadecyl tributyl phosphonium bromide ((C₄)₃C₁₆P⁺ Br[−]).

excellent agreement with X-ray structures of triazole salts, giving bond lengths that are within 0.003 nm of the experimental values in the case of the common 3,4,5-triamino-1,2,3-triazole salts.²⁶ Performing electronic structure calculations on large systems of ionic liquids can be difficult given the fact that *ab initio* electronic structure theory methods scale $\sim N^4$ or worse, depending on the chosen method, where *N* measures the size of the system. This means that correlated electronic structure methods become computationally prohibitive for very large systems with more than 100 heavy atoms. A common approach for large systems is to treat the most important part of the system using quantum mechanics (QM) and the remainder (bulk) using molecular mechanics (MM). These combined QM/MM methods have had some success for large systems. However, not all large species of interest have an obvious separation between QM and MM regions, and the electronic effects of the MM region cannot usually be captured by MM calculations. In such cases, a fully QM treatment is preferable. A fully QM treatment can be made feasible if one can divide (fragment) the system of interest into smaller fragments in such a manner that QM accuracy is retained.^{27,28} For example, the fragment molecular orbital (FMO) method^{28–32} divides the system into fragments and computes each fragment (monomer) in the presence of the electrostatic potential of the other fragments. The FMO method is suited for larger systems and has been applied to systems such as polypeptides and proteins,³³ a heavy metal system containing 3596 atoms,³⁴ and clusters of thousands of water molecules.³⁵

Large systems can be treated at a high level of theory, thereby allowing valuable insight into large systems of ionic liquids. The use of the FMO method with ionic liquid systems³⁶ has been limited and is explored in this report.

Additional studies used to investigate the dynamics of the HEATN system include the use of fluorescence spectroscopy to compare this high-energy ionic liquid to other more commonly used ionic liquids. Steady-state and time-resolved fluorescence measurements were performed to assess how HEATN behaves as a solvent at short time scales. In particular, solvation dynamics experiments were carried out using the fluorescent probe coumarin 153 (C153) in HEATN. The structure of C153 is given in Figure 1c. C153 is an ideal probe and has been used extensively in a large number of solvation dynamics studies in various media.^{37–48} The pervasive use of C153 permits facile comparison of HEATN with other ionic liquid systems. A summary of the various solvation dynamics studies in ionic liquids has recently been published,⁴⁹ as well as a report of some of the applications of such explorations.⁵⁰ Until now there have been no explorations of the solvation dynamics of triazolium ionic liquid systems. The solvation dynamics of the HEATN system were investigated via the C153 probe at five different temperatures, and the rotational dynamics were measured by exploiting the anisotropic nature of the fluorescence of the probe through this viscous ionic liquid as a function of temperature. Comparisons with previously studied imidazolium and phosphonium ionic liquids are presented.

MATERIALS AND METHODS

Computational Methods. Molecular structures were obtained by performing geometry optimizations using second-order Moller–Plesset perturbation theory (MP2)⁵¹ and the 6-31++G(d,p) basis set.^{52,53} Hessians (matrices of the energy second derivatives) were determined to ensure that each stationary point is a minimum (no negative eigenvalues) or a transition state (one negative eigenvalue). All calculations presented in this work are gas-phase cluster calculations. Population analysis was carried out using electrostatic potentials (ESP) following the geodesic approach. Studies of two cation–anion pairs (tetramers) were carried out using the FMO2 and FMO3 method, at the MP2 level of theory.²⁹ In the FMO2 method, all single fragments (monomers) and pairs of fragments (dimers) are calculated explicitly in the electrostatic field of the remainder of the system. The FMO2 energy may be written as $E = \sum_i^N E_i + \sum_{i>j}^N (E_{ij} - E_i - E_j)$, where E_i and E_{ij} are the monomer and dimer energies, respectively.³⁰ Likewise, the FMO3 energy includes the explicit QM calculations of all trimers, so that three-body interactions are included explicitly. The computational efficiency of the FMO method can be exploited by the use of the generalized distributed data interface (GDDI) allowing two levels of parallelism.⁵⁴ With the ionic liquid system studied in this work, each fragment (monomer) was taken to be one cation or one anion. All calculations were performed using the electronic structure theory program GAMESS (General Atomic and Molecular Electronic Structure System)^{55,56} and were visualized when possible with MacMolPlt.⁵⁷

Materials. Coumarin 153 (C153) (Exciton Inc., Dayton, OH) was used as received. 4-Amino-1,2,4-triazole was purchased from Sigma. The production of 1-substituted 4-amino-1,2,4-triazolium nitrate ionic liquid molecules through a metathesis of heterocyclic halide and nitrate salts is well established.^{23,58} The specific synthesis of 1-hydroxyethyl-4-amino-1,2,4-triazolium bromide (HEATB) and 1-hydroxyethyl-4-amino-1,2,4-triazolium nitrate (HEATN) from metathesis of HEATB with silver nitrate follows the procedure described by Drake, Hawkins, and Tollison.⁵⁹

The synthesis of the other ionic liquids shown in Figure 1 is described elsewhere,^{11,60,61} and they were decolorized according to the procedure described previously.⁶² Briefly, the impure ionic liquid was diluted and was allowed to elute through a column packed with celite, silica gel, and activated charcoal. After the excess solvent was removed, the ionic liquid was dried under vacuum with mild heating. The water content of the HEATN sample was determined using a Mettler Toledo DL 39 coulometric Karl Fischer titrator. The viscosity of the HEATN sample was measured at each of the five temperatures ± 0.1 °C using a ViscoLab 4000 viscometer from Cambridge Applied Systems.

Steady-State Measurements. Steady-state absorption spectra were obtained using a Hewlett-Packard 8453 UV–visible spectrophotometer with 1 nm resolution. Steady-state fluorescence measurements were taken using a SPEX fluoromax-4 spectrofluorometer (HORIBA Jobin Yvon) with 1 nm resolution. The emission spectra were corrected for detector response and the lamp spectral intensity. All emission spectra were obtained with an excitation wavelength of 407 nm and a 3 nm band-pass. A 3 mm path length quartz cuvette was used for all measurements.

Time-Resolved Measurements. Fluorescence lifetime measurements were made using the time-correlated single-photon counting (TCSPC) apparatus described previously.^{9,47}

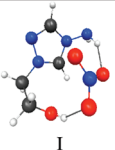
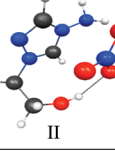
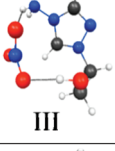
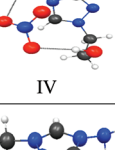
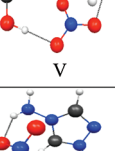
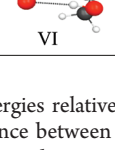
A summary is included here. Using a homemade mode-locked Ti:sapphire oscillator pumped at 532 nm by a Nd:VO₄ Millennia (Spectra-Physics) laser, femtosecond pulses were produced which were tunable from 780 to 900 nm having a repetition rate of 82 MHz. With the output selected at 814 nm from the Ti:Sapphire oscillator, the repetition rate was reduced to 8.8 MHz via the use of a Pockels cell (model 350-160 from Conoptics Inc.) and was subsequently frequency doubled through the use of a harmonic generator (model TP-2000B from U-Oplaz Technologies). The produced blue light with a wavelength of 407 nm was used as the primary excitation source for all time-resolved studies. After the harmonic generator, a half-wave plate was placed in front of a vertical polarizer to ensure the polarization of the excitation light. The fluorescence was collected at a 90° angle to the excitation source and then passed through an emission polarizer set to the magic angle (54.7°) with respect to the vertical excitation light. In the case of the anisotropy studies, this polarizer was set to 0° and 90° with respect to the vertical excitation light, respectively. A 425 nm cutoff filter was placed before a multichannel plate (MCP) (Hamamatsu) to help remove any unwanted scattered excitation light. When performing the solvation dynamics studies, a monochromator was placed before the MCP to ensure the collection at each selected wavelength. The signal from the MCP detector was amplified and sent to a Becker and Hickl photon counting module (model SPC-630). The instrument response function had a full width at half-maximum (fwhm) of ~ 45 –50 ps. The parallel and perpendicular-polarized fluorescence anisotropy decay curves were collected in a 22 ns time window and fitted simultaneously following the method described by Cross and Fleming.⁶³ This method takes full advantage of the statistical properties of the measured curves. The solvation dynamics studies involved recording 15 single wavelength decays from 490 to 630 nm in 10 nm intervals, in a time window of 9 ns. Typically, 1024 channels of data were collected giving 8.8 ps/channel. The wavelength-resolved fluorescence transients were fit to sums of exponentials (typically 2 or 3, as necessary to fit the data), and time-resolved emission spectra (TRES) were reconstructed as described in previous reports.^{9,47}

The traditional approach was used for fitting the time-resolved emission spectra to a log-normal function,^{9,37,61} from which the peak frequency $\nu(t)$ is extracted as a function of time. The solvation dynamics is described by the following normalized correlation function

$$C(t) = \frac{\nu(t) - \nu(\infty)}{\nu(0) - \nu(\infty)} \quad (1)$$

Because $C(t)$ is a *normalized* function, the accurate determination of $C(t)$ depends upon accurate values for $\nu(0)$ and $\nu(\infty)$. $\nu(0)$ is the frequency at zero time, estimated using the method of Fee and Maroncelli,⁶⁴ who have described a robust, model independent, and simple procedure for generating this “zero-time” spectrum. $\nu(0)$ represents the emission spectrum expected prior to any solvent relaxation but after complete intramolecular vibrational redistribution. The validity of this approach has been checked using a different method for estimating the zero-time reorganization energy in a previous report⁶⁰ and was shown to be reliable. $\nu(\infty)$ is (usually^{65,66}) the frequency at infinite time, obtained from the maximum of the steady state spectrum. (This is not, however, true in the case of very slowly relaxing solvents, as has been demonstrated in the

Table 1. MP2 Dimer HEATN Properties.

Dimer ^a	E _{rel} ^b (kcal/mol)	OH...O ^b (Å)	NH...O ^b (Å)	ESP Charges (cation, anion) ^c
 I	0	1.85	1.90	0.82, -0.82
 II	0.6	1.84	1.96	0.79, -0.79
 III	3.3	1.87	1.93	0.83, -0.83
 IV	3.6	1.88	1.91	0.80, -0.80
 V	4.0	1.84	1.93	0.80, -0.80
 VI	5.0	1.86	1.84	0.82, -0.82

^a Energies relative to dimer "I". ^b OH...O and NH...O refer to the distance between the OH/NH group on the cation and the nearest O atom on the anion. ^c Electrostatic Potential (ESP) charges on each cation and anion are reported listing the cation first and the anion second. ^d MP2 optimized dimer structures of HEATN using the 6-31++G(d,p) basis arranged in order of increasing energy with "I" being the lowest-energy structure found. The atom color codes are: nitrogen is blue, oxygen is red, carbon is black, and hydrogen is white.

case of certain ionic liquids,^{11,65,66} for which the emission spectrum at ~ 3 times the fluorescence lifetime of the probe is *red-shifted* to that of the equilibrium spectrum.) The $\nu(t)$ values are determined from the maxima of the log-normal fits of the time-resolved emission spectra. In most of the cases, however, the spectra are broad, so there is some uncertainty in the exact position of the emission maxima. Thus, the range of the raw data points in the neighborhood of the maximum needed to estimate an error for the maximum obtained from the log-normal fit was considered. Depending on the width of the spectrum (i.e., zero-time, steady-state, or time-resolved emission spectrum), the typical uncertainties were determined to be: zero-time \sim steady-state ($\sim \pm 100 \text{ cm}^{-1}$) $<$ time-resolved emission ($\sim \pm 200 \text{ cm}^{-1}$). These uncertainties were used to compute error bars for the $C(t)$ graph (giving a maximum error of ± 0.04). Finally, in generating the $C(t)$ curve, the first point was obtained from the zero-time spectrum. The second point was taken at the maximum of the instrument response function. The fractional

solvation was also computed at 50 ps by taking $f_{50\text{ps}} = 1 - C(t = 50 \text{ ps})$. The experiments were also carried out at five different temperatures (25, 35, 45, 55, and 65 °C) that were obtained using a variable-temperature sample cell holder.

RESULTS AND DISCUSSION

HEATN Structures. A previous *ab initio* investigation¹⁸ of triazolium ionic liquid systems, especially triazolium dinitramide, showed a tendency for proton transfer from the cation to the anion in an ionic dimer to form neutral pairs. This proton transfer was found to have a very low energy barrier and was often spontaneous. This tendency was investigated for the HEATN system by performing geometry optimizations on the different pairs of cations and anions. The geometric structures of both single cation–anion pairs (dimers) and two cation–anion pairs (tetramers) were investigated. Six structures labeled I, II, III, IV, V, and VI were found for the HEATN dimer (Table 1) at the MP2 level of theory. These structures are ordered with respect to their relative energies with structure "I" having the lowest energy. The relative energies are given in Table 1, along with the hydrogen bond distances and the electrostatic potential derived charges. Interestingly, no spontaneous proton transfer from the cation to the anion ions is found to occur. The magnitudes of the charges are ~ 0.8 in each structure, so these are clearly ionic species. There are two hydrogen bonds, OH...O and NH...O, that connect each cation–anion pair. The corresponding hydrogen bond distances are listed in Table 1. The hydrogen bonds may contribute to a larger density than these species might otherwise have. High density is a desirable property of high-energy species.⁶⁷

The HEATN tetramer was also investigated using the MP2 method. Each tetramer structure was found by taking the dimer geometries and combining them to form tetramers. The MP2 geometry optimizations using these starting structures yielded the five geometries seen in Figure 2. The relative energies, hydrogen bond distances, and the electrostatic potential derived charges are given in Table 2.²⁷ The computed charges are all above 0.7 in magnitude, so that all of the species are ionic as expected.

The FMO method was used to evaluate the feasibility of using this method with larger (hexamer and higher) ionic liquid clusters. The structures discussed above provide benchmarks against which the FMO2-MP2 and the FMO3-MP2 method may be compared, as shown in Table 3. For each system, one molecule was assigned to each fragment, giving one ion per FMO monomer. As expected, the FMO3-MP2 method has smaller errors, but both FMO2 and FMO3 are within 1 kcal/mol or less of the full MP2 relative energies. Thus, the less computationally demanding FMO2 method provides sufficient accuracy for these species, suggesting that three-body effects are minor. Of equal importance is the memory required for the calculations. The full MP2 method uses 8.00 GB of RAM per node of eight cores, while the FMO2-MP2 and FMO3-MP2 methods use 1.93 and 1.12 GB, respectively. The ESP charges derived from the FMO2 and FMO3 single-point calculations are in good agreement with the MP2 values (see Table 3).

Solvation Dynamics of C153 in HEATN. HEATN was investigated using the fluorescent probe molecule C153. The absorption and emission spectrum maximum is at 431 and 546 nm, respectively, and there was no temperature-dependent shift of the spectra of C153 in HEATN. The fluorescence of C153 underwent a monotonic red shift depending upon the

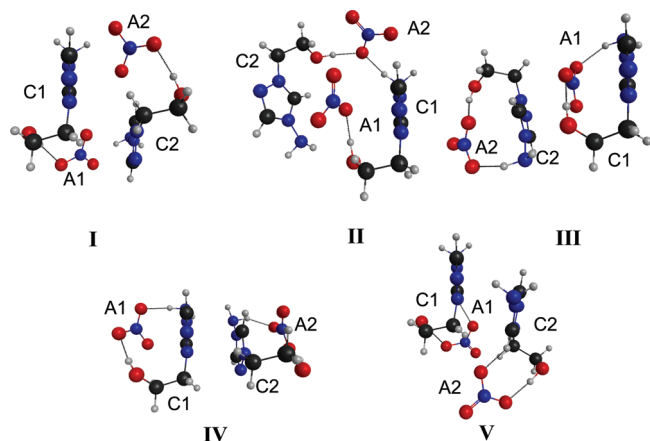


Figure 2. Tetramer structures of HEATN obtained using the MP2 method with the 6-31++G(d,p) basis. They are labeled in order of increasing energy. Red represents oxygen, blue represents nitrogen, black represents carbon, and white represents hydrogen. Additional data obtained from these calculations can be seen in Tables 2 and 3.

Table 2. MP2 Optimized HEATN Tetramers (see Figure 2)

tetramer	E_{rel}^a (kcal/mol)	ion ^b	NH...O ^c (Å)	OH...N ^c (Å)	ESP charge
I	0.0	C1	2.00	1.84	0.86
		A1			−0.86
		C2	2.00	1.84	0.86
		A2			−0.86
II	10.1	C1	1.77	1.70	0.86
		A1			−0.74
		C2	1.73	2.45	0.78
		A2			−0.91
III	18.8	C1	1.93	1.78	0.93
		A1			−0.92
		C2	1.88	1.89	0.82
		A2			−0.84
IV	27.8	C1	1.89	1.81	0.81
		A1			−0.78
		C2	1.86	1.80	0.73
		A2			−0.76
V	39.4	C1	5.05	1.73	0.95
		A1			−0.90
		C2	4.74	1.75	0.83
		A2			−0.88

^a Energies (kcal/mol) relative to tetramer “I”. ^b These ions are defined in Figure 2. ^c OH...O and NH...O refer to the distance between the OH/NH group on the cation and the nearest O atom on the associated anion (see Figure 2).

increase in excitation wavelength from 400 to 500 nm. The excitation wavelength dependence, or red edge excitation effect, has also been observed in other ionic liquids.^{68,69} This effect observed in ionic liquids is due to its inherent heterogeneity. The observed heterogeneity is attributed to the presence of nano-structural assemblies and different microenvironments within the neat ionic liquid.^{70,71} Thus, exciting at different wavelengths selectively excites molecules in different local environments, and thus the solvent response around the excited probe differs from

one to another. To construct the solvation correlation function $C(t)$, time-resolved fluorescence decays were collected at different wavelengths spanning the entire range of the emission spectrum of the probe as shown in Figure 3. The decays on the blue end of the spectrum are characterized by a faster response, whereas those collected at longer wavelengths are accompanied by a rise time that was due to the population flux from the initially excited state to the relaxed state. This trend of wavelength-dependent decays is a signature of local solvation dynamics. Time-resolved emission spectra at 50 ps and 7.05 ns of C153 in HEATN are presented in Figure 4 at two representative temperatures. The corresponding steady-state and zero-time spectra are also included. Note that unlike the spectrum at 55 °C the 7.05 ns spectrum crosses the steady-state spectrum at 25 °C, indicating that this spectrum cannot be interpreted to convey adequately the completed solvation of C153, as would usually be expected for highly viscous solvents.^{11,65,66} The spectrum recorded at 7.05 ns is red-shifted by $\sim 270 \text{ cm}^{-1}$ relative to the steady-state spectrum, demonstrating that solvation is slightly slower than the population decay of the S_1 state of C153. This phenomenon has been previously observed in the case of the slowly relaxing phosphonium ionic liquids. In previous studies,¹¹ it was found that the amount of rapid solvation and the average solvation time decrease and increase, respectively, as the time window of the experiment is increased. The occurrence of solvation that is slower than the population decay of the S_1 state has also been noticed elsewhere for related systems.^{65,66} To compare the solvation in the ionic liquid media, an attempt was made to study the parent compound (Figure 1b) which is the neutral 4-amino-1,2,4-triazole (melting point $\sim 85^\circ\text{C}$). A solvent-induced spectral shift was not observed in the molten state at 85 °C using the time resolution afforded by our TCSPC apparatus, suggesting a very fast response for the triazole, which is consistent with the low viscosity ($\sim 6.2 \text{ cP}$) of the triazole at the melting temperature.

The spectral shift dynamics are represented by the decay of the solvation correlation function $C(t)$ in Figure 5. The $C(t)$ values are constructed at five temperatures (25, 35, 45, 55, and 65 °C), and the solvation parameters can be seen in Table 4. At all temperatures, the solvation dynamics are well described by biphasic decays, with an initial faster component preceded by a slower response. At 25 °C, $\sim 30\%$ of the solvation is completed within the instrumental time resolution ($\sim 50 \text{ ps}$). The fractional solvation, $f_{50\text{ps}}$, listed in Table 4 is the solvent response that is missed due to the finite time resolution of the TCSPC apparatus. The missing Stokes shift was accounted for by using the zero-time spectra estimated by the method of Fee and Maroncelli.⁶⁴ Recently, Kerr-gated emission (KGE)^{72,73} and fluorescence upconversion techniques^{74,75} were used to measure spectral dynamics in ionic liquids with much shorter time resolution ranging from 200 to 500 fs. Both the Maroncelli and Vauthey groups have reported a small but significant amount of a sub-picosecond component in the case of solvation in ionic liquids. Maroncelli and co-workers have used a combination of KGE and TCSPC data to resolve complete solvation response in ionic liquids using 4-dimethylamino-4'-cyanostilbene (DCS) as a probe.^{72,73} The observed response functions were well described by biphasic decays, consisting of both a subpicosecond component of $\sim 10\text{--}20\%$ amplitude and a dominant slower component relaxing over a few picoseconds up to several nanoseconds. The faster component was associated with the inertial characteristics of the constituent ions and the slower component to solvent

Table 3. Comparison of MP2 and FMO-MP2 for the Tetramer Geometries in Figure 2

tetramer	E_{rel}^a (kcal/mol)			ion ^b	FMO2-MP2	FMO3-MP2
	MP2	FMO2-MP2 error ^c	FMO3-MP2 error ^d		ESP charge	ESP charge
I	0.00	−0.30	0.02	C1	0.93	0.83
				A1	−0.93	−0.83
				C2	0.94	0.83
				A2	−0.93	−0.83
II	10.13	0.63	0.02	C1	0.97	0.92
				A1	−0.80	−0.78
				C2	0.87	0.82
				A2	−1.03	−0.96
III	18.76	0.55	−0.09	C1	0.85	0.91
				A1	−0.92	−0.88
				C2	0.93	0.81
				A2	−0.86	−0.84
IV	27.75	0.98	−0.28	C1	0.80	0.75
				A1	−0.78	−0.73
				C2	0.74	0.68
				A2	−0.77	−0.71
V	39.43	0.40	0.13	C1	1.01	0.93
				A1	−0.93	−0.89
				C2	0.91	0.83
				A2	−0.99	−0.86

^a E_{rel} reports the energies (kcal/mol) relative to tetramer “I”. ^b These ions are defined in Figure 2. ^c The FMO2-MP2 energy error relative to the MP2 energy. ^d The FMO3-MP2 energy error relative to the MP2 energy.

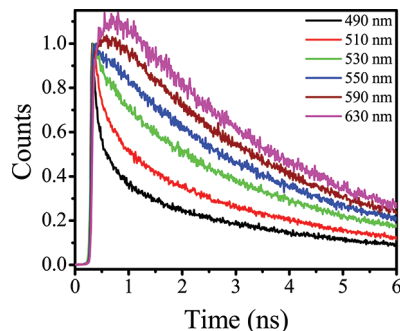


Figure 3. Representative normalized wavelength-resolved fluorescence decay traces of C153 at six different wavelengths in HEATN at 55 °C.

viscosity. The missing portion of the initial relaxation contains both subpicosecond inertial contributions as well as components relaxing on the 1–10 ps time scale,⁷³ and this interpretation was also corroborated by simulations performed by Kobrak.⁷⁶

As expected, the solvation times decreased with increasing temperature. This was most likely because of the decrease in the viscosity of the ionic liquid which allowed the neighboring solvent molecules to reorganize faster around the excited state dipole of C153. Figure 6a shows the dependence of solvation time on viscosity in different types of ionic liquids, namely, those based on imidazolium, phosphonium, and triazolium cations. The solvation times of C153 in HEATN show a reasonable correlation with viscosity, whereas in imidazolium-based ionic liquids the correlation is not as good. Marked deviations are observed for the case of phosphonium ionic liquids. This observation is consistent with those reported by Maroncelli

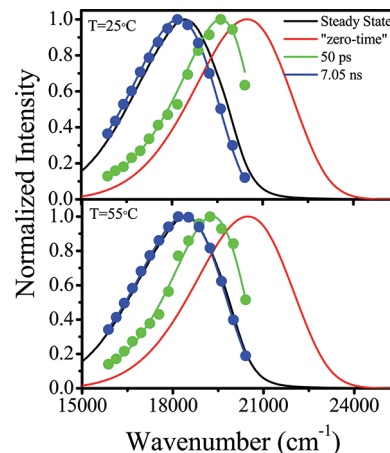


Figure 4. Time-resolved fluorescence emission spectra (TRES) of C153 in HEATN at 25 °C (top panel) and 55 °C (bottom panel) at 50 ps and 7.05 ns. Corresponding steady-state and time-zero spectra are also included. The error for the steady-state and time-zero spectra is $\sim \pm 100 \text{ cm}^{-1}$, while for the other timed points it was $\sim \pm 200 \text{ cm}^{-1}$.

and co-workers,^{66,77} who attributed the deviations in phosphonium ionic liquids to the enormous size of the cation moiety. Solvation in phosphonium ionic liquids is much slower than that of the imidazolium and HEATN systems. For example, although $(\text{C}_6)_3\text{C}_{14}\text{P}^+ \text{Br}^-$ ⁷⁷ is isoviscous ($\sim 270 \text{ cP}$) with HEATN (at 35 °C), the solvation is 5 times slower in the phosphonium liquid. This observation can be interpreted in terms of the van der Waals volumes of the constituent ions. The radii of the cations and anions listed in Table 4 were estimated using Edward's⁷⁸ and

Bondi's⁷⁹ van der Waals increment methods. The radii decrease in the order of phosphonium (~ 5.3 Å) > imidazolium (~ 3.4 Å) > triazolium (~ 2.9 Å). This probably also explains the 2-fold faster average solvation times in HEATN compared to the isoviscous imidazolium-based ionic liquids. It is noteworthy in this context that in all of the imidazolium-based ionic liquids studied so far the completely relaxed state or equilibrium condition is represented adequately by the steady-state spectrum of the probe; however, this was not the case in HEATN under ambient temperature.

As discussed above, besides viscosity (η), the size of the individual ions strongly influences the solvent response. To elucidate how the ion size might affect the observed solvation times, different analyses were performed motivated by the methods of Maroncelli and co-workers.⁷⁷ The ion sizes were correlated to the logarithm of the solvation times (τ_s) and to various measured and calculated properties. A plot of $\log \langle \tau_s \rangle$ versus η/T did not provide substantial improvement compared to a plot of $\log \langle \tau_s \rangle$ against η only. Consistent with the reports of Jin et al.,⁷⁷ a much better correlation was found, as

shown in Figure 6b, in which the solvation time varies as $(\eta/T)^{A R_+^B}$, where R_+ is the radius of the cation and A and B are constants determined to be 0.5 and 4.5 by multiple regression analysis. This correlation was slightly improved when the anion size (R_-) is incorporated as shown in Figure 6c. Thus, the dependence of solvation time could be best described as follows

$$\langle \tau_s \rangle \propto \sqrt{\frac{\eta/T}{R_-}} R_+^{4.5} \quad (2)$$

The diffusion times of the cation and anion of HEATN, which is the amount of time needed to move a root-mean-square distance equal to the radius of the liquid, were calculated using the relation $t_{\pm} = \eta R_{\pm}^3 / f_{\pm} k_B T$, where k_B is the Boltzmann constant and f is an empirical correction factor,^{80,81} 0.53 and 0.74⁸² for '+' and '-' which refer to the cation and anion, respectively. The calculated diffusion times are presented in Table 4. The correlation of solvation time with the diffusion time of the cation and anion, as shown in Figure 7, indicates that the contribution of the reorientational motion of ions to the overall relaxation process cannot be neglected.

Rotational Dynamics of C153 in HEATN. The fluorescence anisotropy of C153 in HEATN was measured at five different temperatures and was found to decrease with temperature. The anisotropy decay was nonexponential at all temperatures investigated, unlike in normal polar solvents. The limiting anisotropy (r_0) and rotational times are presented in Table 4. Figure 8 gives the variation of rotational time (τ_{rot}) of C153 in HEATN as a function of viscosity and temperature in the form of η/T . This plot shows a good correlation in the form $\langle \tau_{\text{rot}} \rangle \propto A(\eta/T)^{0.8}$, where A is a constant determined from the linear fit to be 1.1. Ionic liquids have been reported to show similar correlation as established by normal polar solvents.⁷⁷

The experimentally measured anisotropy decay times of C153 in HEATN have been analyzed within the framework of Stokes–Einstein–Debye (SED) hydrodynamic theory. According to this theory, the rotational diffusion of a medium-sized solute molecule in a solvent continuum is assumed to occur by small step diffusion and the reorientation time of the solute and is related to the macroscopic

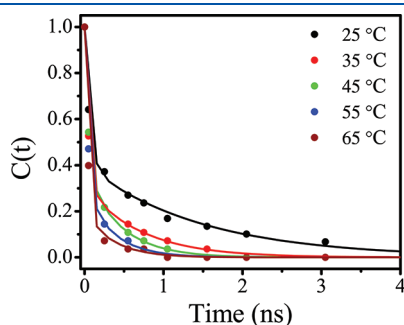


Figure 5. Solvation correlation function ($C(t)$) decay curves of C153 in HEATN plotted as a function of temperature. The decays were fit with two exponentials, and the average solvation time as well as the fractional solvation values can be found in Table 4. The typical error for each data point is <0.05 . Water content was determined to be <0.3 wt %.

Table 4. Solvation and Anisotropy Parameters in Different Ionic Liquids

ionic liquid	T (K)	η^a (cP)	R_+^b (Å)	R_-^c (Å)	anisotropy ^d			solvation			
					r_0	$\langle \tau_{\text{rot}} \rangle$ (ns)	C_{rot}^e	f_{obs}^f	$\langle \tau_{\text{solv}} \rangle^g$ (ns)	t_+^h (ns)	t_-^h (ns)
HEATN	298	427	2.90	2.09	0.35 ± 0.03	21.1 ± 0.6	0.48	0.36	0.62	4.7	1.3
	308	272			0.36 ± 0.10	11.3 ± 0.5	0.42	0.47	0.22	2.9	0.70
	318	133			0.32 ± 0.02	5.7 ± 0.4	0.45	0.45	0.16	1.4	0.30
	328	69			0.38 ± 0.02	4.3 ± 0.7	0.67	0.53	0.10	0.7	0.18
	338	40			0.36 ± 0.01	2.6 ± 0.1	0.72	0.60	0.07	0.4	0.10
BMIM Cl ⁱ	343	334	3.29	2.09				0.21	0.59		
BIM NTf ₂ ⁱ	293	90	3.16	3.39				0.65	0.20		
MIM NTf ₂ ⁱ	293	77	2.69	3.39				0.64	0.42		
CVIM NTf ₂ ^j	342	38	4.05	3.39				0.62	0.28		
P(C ₄) ₃ C ₁₆ Br ^k	339	268	4.96	2.26				0.29	5.3		
P(C ₆) ₃ C ₁₄ Cl ^k	331	80	5.18	2.09				0.33	3.9		

^a Error bars for viscosity measurements are within ± 1 –2%. ^b van der Waals volumes of the cations (V_w) are calculated from Edward's atomic increments,⁷⁸ and the radius of cations (R_+) is obtained using the relation $R_+ = (3V_w/4\pi)^{1/3}$. ^c Radius of anions (R_-) is obtained from Bondi⁷⁹ and Jin et al.⁷⁷ ^d The error bars in the anisotropy experiments are obtained from triplicate measurements. ^e Rotational decoupling constant (C_{rot}) is calculated using eq 4. ^f Fractional solvation, f_{obs} , is calculated at 50 ps for HEATN samples and 100 ps for other ionic liquids. ^g Average solvation times $\langle \tau_{\text{solv}} \rangle$ are obtained by the fitting $C(t)$ curves with two exponentials. ^h The cation (t_+) and anion (t_-) diffusion times are calculated using the equation $t_{\pm} = \eta R_{\pm}^3 / f_{\pm} k_B T$, where the parameters are defined in the text. ⁱ From ref 60. ^j From ref 61. ^k From ref 11.

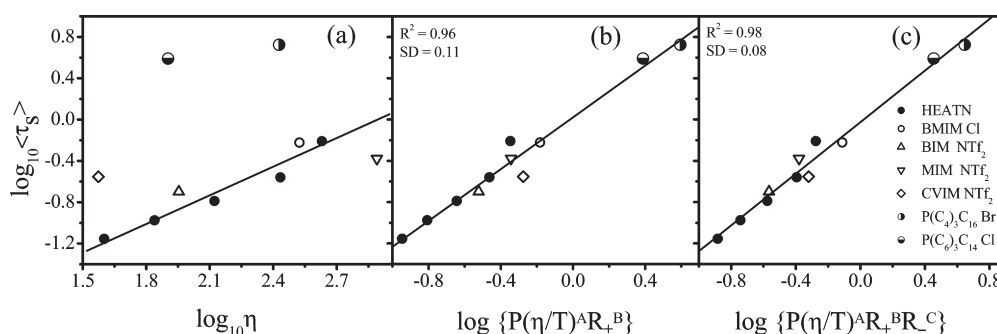


Figure 6. (a) Average solvation time ($\langle \tau_s \rangle$) of C153 is plotted as a function of viscosity (η) in different ionic liquids based on imidazolium, phosphonium, and triazolium cations. The solvation times of C153 in HEATN show a reasonable correlation with viscosity, whereas in imidazolium and phosphonium ionic liquids studied previously poor agreement is seen. The straight line is drawn to help guide the eye. (b) Correlation of $\langle \tau_s \rangle$ in the ionic liquids with η/T and cation radius (R_+). The proportionality of $\langle \tau_s \rangle$ varies as $(\eta/T)^A R_+^B$, where R_+ is the radius of the cation, and A and B are constants determined to be 0.5 and 4.5 by multiple regression analysis. This correlation is slightly improved when the anion size (R_-)^{-0.5} is incorporated (c). The R^2 and standard deviation (SD) are obtained from the fit represented by the straight line in (b) and (c).

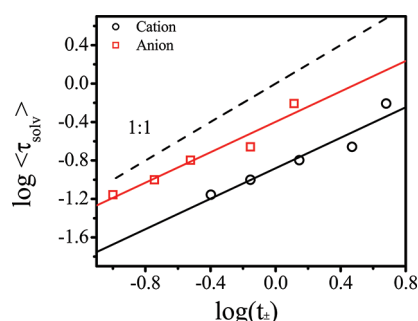


Figure 7. Solvation times of C153 in HEATN at five different temperatures versus estimates of the cation and anion diffusion time determined using the equation $t_{\pm} = \eta R_{\pm}^3 / f_{\pm} k_B T$, where the parameters are defined in the text. The linear fits are shown as solid straight lines, whereas the dashed line represents the 1:1 correlation.

viscosity of the solvent by the following relation^{83,84}

$$\tau_{hyd} = \frac{V\eta}{k_B T} fC \quad (3)$$

The dashed lines in Figure 8 are the predictions of hydrodynamic models, made by assuming C153 has ellipsoidal shape with semiaxis dimensions of 2.0, 4.8, and 6.1 Å.⁸⁵ In eq 3, V is the van der Waals volume (246 Å³) of the solute; f is a shape factor (1.71); and C is a “rotational coupling factor” which measures the extent of coupling between the solute and the solvent. For stick boundary conditions $C = 1$, and for slip boundary conditions $C = 0.24$.⁸⁵ All of the rotation times in HEATN measured at different temperatures fall between these two limiting predictions. Deviations from the hydrodynamic predictions can be estimated from the value of the rotational coupling factor (C_{rot}) using the relation

$$C_{rot} = \frac{k_B T}{V\eta f} = \frac{\langle \tau_{rot} \rangle}{\tau_{stick}} \quad (4)$$

where τ_{stick} is the stick hydrodynamic prediction. The values of C_{rot} are listed in Table 4. The average value in HEATN is 0.55, whereas those in conventional polar solvents were reported to be 0.57 ± 0.09 .⁷⁷ Thus the coupling of solute and solvent between C153 and HEATN is reasonably comparable to conventional polar solvents. These results are consistent with those of Maroncelli and co-workers

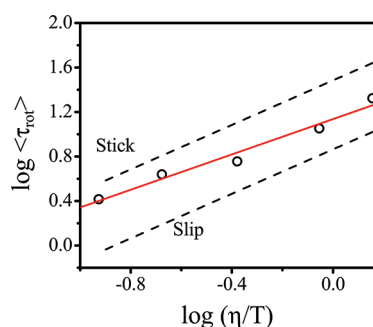


Figure 8. Correlation of the average rotational time ($\langle \tau_{rot} \rangle$) of C153 in HEATN with viscosity (η/cP) and temperature (T/K). The solid line (red) shows the best fit of the data to the proportionality $\langle \tau_{rot} \rangle = 1.13 \times 10^{-9} (\text{sKcP}^{-1}) (\eta/T)^{0.8}$. The dashed lines are the average rotational times predicted from hydrodynamic models assuming an ellipsoidal shape of C153⁸⁵ using “stick” and “slip” boundary conditions. The experimentally observed rotational times fall within the boundaries of hydrodynamic predictions, and the deviations can be estimated by the rotational coupling factor (C_{rot}) as described in the text.

who reported that all ionic liquids, besides bulky ones based on phosphonium, fall within the scatter of the polar solvents.⁷⁷ Cadena and Maginn⁸⁶ have shown via molecular dynamics studies that the rotational time correlation of triazolium systems shows a strong temperature dependence. As the temperature rises the rotational motion increases; this is consistent with the data presented here. Castner and co-workers⁸⁷ have recently studied solvation and rotational dynamics using C153 over a range of temperatures from 5 to 80 °C, in ionic liquids based on ammonium and pyrrolidinium cations. They reported small amplitudes of very long orientation relaxation time constants on the order of 100 ns, which were missing in the experiments reported on herein. All of the C153 rotational time constants in HEATN ranged from 2 to 20 ns and are in agreement with the reports by Maroncelli and co-workers.⁷⁷ The dynamics reported in the time scale of 100 ns may be unreliable where the lifetime of C153 is ~ 3 –5 ns owing to the lack of sufficient photons at long times.

CONCLUSIONS

The structure and dynamics of the high-energy ionic liquid system, 1-hydroxyethyl-4-amino-1,2,4-triazolium nitrate (HEATN),

were investigated. This system maintains a significant charge separation as demonstrated by the electrostatic potential derived charges. There were no instances in which proton transfer was found to occur without an energy barrier, in contrast to other reports on triazolium ionic liquids.¹⁸ The MP2 level optimizations find six dimer and five tetramer structures and show a significant, highly hydrogen bonded network within HEATN. The FMO method adequately treats this ionic liquid system, as evidenced by the small relative errors in the relative energies. Further calculations using the FMO method on the HEATN ionic liquid system are expected to give similar accuracy while using less computer resources and avoiding the prohibitive scaling of traditional full ab initio methods.

Besides the structural characterization, thorough temperature-dependent studies of the solvation and rotational dynamics in HEATN using C153 as a probe were undertaken and compared with the results previously obtained from earlier studies on imidazolium and phosphonium ionic liquids. The solvation time in HEATN is faster than the isoviscous imidazolium and phosphonium ionic liquids, probably due to the smaller size of the cationic moiety. The solvation times in HEATN show an excellent correlation with viscosity and the ionic radii. The fluorescence depolarization studies showed that the rotational time of C153 in HEATN at different temperatures lies within the limits of hydrodynamic predictions. The presence of the amino and hydroxyethyl groups allows HEATN to participate in significant hydrogen bonding interactions. Surprisingly, these interactions do not seem to produce a substantial difference in the dynamics of the HEATN system with respect to imidazolium systems. An exception is given in Figure 6a, where HEATN shows a linear correlation with a significant difference in slope compared to the imidazolium and phosphonium systems. Despite the inherent difference of having the additional nitrogen atom in the ring, no significant changes in the dynamics of this system were observed. Finally, to the authors' knowledge this is the first experimental study of solvation dynamics in a triazolium-based ionic liquid.

AUTHOR INFORMATION

Corresponding Author

*E-mail: mark@si.msg.chem.iastate.edu; jwp@iastate.edu.

ACKNOWLEDGMENT

The authors acknowledge Dr. Gregory Drake, Mr. Michael Tinnirello, Ms. Leslie Hudgens, and Mr. Spencer Pruitt for many helpful discussion and guidance. This work was supported by a grant from the Air Force Office of Scientific Research. S.B. was supported by the U.S. Department of Energy, Office of Basic Energy Sciences, Division of Chemical Sciences, Geosciences, and Bioscience through the Ames Laboratory (S.B.). The Ames Laboratory is operated for the U.S. Department of Energy by Iowa State University under Contract No. DE-AC02-07CH11358.

REFERENCES

- (1) Deetlefs, M.; Hakala, U.; Seddon, K. R.; Wahala, K. *Ionic Liquids IV: Not just solvents anymore*; ACS: Washington, D.C., 2007.
- (2) Earle, M. J.; Seddon, K. R. *Pure Appl. Chem.* **2000**, *72*, 1391.
- (3) Brennecke, J. F.; Maginn, E. J. *AIChE* **2001**, *47*, 2384.
- (4) Forsyth, S. A.; Pringle, J. M.; MacFarlane, D. R. *Aust. J. Chem.* **2004**, *57*, 113.

- (5) Krossing, I.; Slattery, J. M.; Dagueuet, C.; Dyson, P. J.; Oleinikova, A.; Weingartner, H. *J. Am. Chem. Soc.* **2006**, *128*, 13427.
- (6) Seddon, K. R. *Nature (Materials)* **2003**, *2*, 363.
- (7) Anderson, J. L.; Ding, J.; Welton, T.; Armstrong, D. W. *J. Am. Chem. Soc.* **2002**, *124*, 14247.
- (8) Welton, T. *Chem. Rev.* **1999**, *99*, 2071.
- (9) Chowdhury, P. K.; Halder, M.; Sanders, L.; Calhoun, T.; Anderson, J. L.; Armstrong, D. W.; Song, X.; Petrich, J. W. *J. Phys. Chem. B* **2004**, *108*, 10245.
- (10) Adhikary, R.; Bose, S.; Mukherjee, P.; Thite, A.; Kraus, G. A.; Wijeratne, A. B.; Sharma, P.; Armstrong, D. W.; Petrich, J. W. *J. Phys. Chem. B* **2008**, *112*, 7555.
- (11) Mukherjee, P.; Crank, J. A.; Sharma, P. S.; Wijeratne, A. B.; Adhikary, R.; Bose, S.; Armstrong, D. W.; Petrich, J. W. *J. Phys. Chem. B* **2008**, *112*, 3390.
- (12) Bose, S.; Wijeratne, A. B.; Thite, A.; Kraus, G. A.; Armstrong, D. W.; Petrich, J. W. *J. Phys. Chem. B* **2009**, *113*, 10825.
- (13) Hu, Z.; Margulis, C. J. *Acc. Chem. Res.* **2007**, *40*, 1097.
- (14) Rogers, R. D.; Voth, G. A. *Acc. Chem. Res.* **2007**, *40*, 1077.
- (15) Bose, S.; Armstrong, D. W.; Petrich, J. W. *J. Phys. Chem. B* **2010**, *114*, 8221.
- (16) Bose, S.; Barnes, C. A.; Petrich, J. W. *Biotechnol. Bioeng.* **2012**, *109*, 434.
- (17) Fischer, G.; Holl, G.; Klapötke, T. M.; Weigand, J. J. *Thermochim. Acta* **2005**, *437*, 168.
- (18) Schmidt, M. W.; Gordon, M. S.; Boatz, J. A. *J. Phys. Chem. A* **2005**, *109*, 7285.
- (19) Zorn, D. D.; Boatz, J. A.; Gordon, M. S. *J. Phys. Chem. B* **2006**, *110*, 11110.
- (20) Pimienta, I. S. O.; Elzey, S.; Boatz, J. A.; Gordon, M. S. *J. Phys. Chem. A* **2007**, *111*, 691.
- (21) Singh, R. P.; Verma, R. D.; Meshri, D. T.; Shreeve, J. M. *Angew. Chem.* **2006**, *45*, 3584.
- (22) Drake, G.; Hawkins, T.; Brand, A.; Hall, L.; McKay, M.; Vij, A.; Ismail, I. *Propellants, Explos., Pyrotech.* **2003**, *28*, 174.
- (23) Drake, G.; Hawkins, T.; Tollison, K.; Hall, L.; Vij, A.; Sobaski, S. (1R)-4-Amino-1,2,4-triazolium Salts: New Families of Ionic Liquids; ACS Symp. Ser. 902; ACS: Washington D.C., 2005.
- (24) Jiang, W.; Yan, T.; Wang, Y.; Voth, G. A. *J. Phys. Chem. B* **2008**, *112*, 3121.
- (25) Wasserscheid, P.; Keim, W. *Angew. Chem., Int. Ed.* **2000**, *39*, 3772.
- (26) Drake, G.; Hawkins, T.; Hall, L.; Boatz, J. A.; Brand, A. *Propellants, Explos., Pyrotech.* **2005**, *30*, 329.
- (27) Gordon, M. S.; Mullin, J. M.; Pruitt, S. R.; Roskop, L. B.; Slipchenko, L. V.; Boatz, J. A. *J. Phys. Chem. B* **2009**, *113*, 9646.
- (28) Fedorov, D. G.; Kitaura, K. *J. Phys. Chem. A* **2007**, *111*, 6904.
- (29) Fedorov, D. G.; Kitaura, K. Theoretical Background of the Fragment Molecular Orbital Method. In *The Fragment Molecular Orbital Method - Practical Applications to Large Molecular Systems (FMO) Method and Its Implementation in GAMESS*; Fedorov, D. G., Kitaura, K., Eds.; CRC Press: Boca Raton, FL, 2009; p 5.
- (30) Fedorov, D. G.; Kitaura, K. Theoretical Development of the Fragment Molecular Orbital (FMO) Method. In *Modern Methods for Theoretical Physical Chemistry of Biopolymers*; Starikov, E. B., Lewis, J. P., Tanaka, S., Eds.; Elsevier: Amsterdam, 2006; p 3.
- (31) Kitaura, K.; Ikeo, E.; Asada, T.; Nakano, T.; Uebayasi, M. *Chem. Phys. Chem. Lett.* **1999**, *313*, 701.
- (32) Nakano, T.; Kaminuma, T.; Sato, T.; Fukuzawa, K.; Akiyama, Y.; Uebayasi, M.; Kitaura, K. *Chem. Phys. Lett.* **2002**, *351*, 475.
- (33) Fedorov, D. G.; Ishida, T.; Uebayasi, M.; Kitaura, K. *J. Phys. Chem. A* **2007**, *111*, 2722.
- (34) Ishikawa, T.; Mochizuki, Y.; Nakano, T.; Amari, S.; Mori, H.; Honda, H.; Fujita, T.; Tokiwa, H.; Tanaka, S.; Komeiji, Y. *Chem. Phys. Lett.* **2006**, *427*, 159.
- (35) Fletcher, G. D.; Fedorov, D. G.; Pruitt, S. R.; Windus, T. L.; Gordon, M. S. *J. Chem. Theory. Comput.* **2011**, in press.
- (36) Pruitt, S. R.; Gordon, M. S., In preparation.
- (37) Maroncelli, M.; Fleming, G. R. *J. Chem. Phys.* **1987**, *86*, 6221.

- (38) Horng, M. L.; Gardecki, J. A.; Papazyan, A.; Maroncelli, M. *J. Phys. Chem.* **1995**, *99*, 17311.
- (39) Lewis, J. E.; Maroncelli, M. *Chem. Phys. Lett.* **1998**, *282*, 197.
- (40) Changuenet-Barret, P.; Choma, C. T.; Gooding, E. F.; DeGrado, W. F.; Hochstrasser, R. M. *J. Phys. Chem. B* **2000**, *104*, 9322.
- (41) Jiang, Y.; McCarthy, P. K.; Blanchard, D. J. *Chem. Phys.* **1994**, *183*, 249.
- (42) Palmer, P. M.; Chen, Y.; Topp, M. R. *Chem. Phys. Lett.* **2000**, *318*, 440.
- (43) Chen, Y.; Palmer, P. M.; Topp, M. R. *Int. J. Mass Spectrom.* **2002**, *220*, 231.
- (44) Agmon, N. *J. Phys. Chem.* **1990**, *94*, 2959.
- (45) Chakraborty, D.; Hazra, P.; Chakraborty, A.; Seth, D.; Sarkar, N. *Chem. Phys. Lett.* **2003**, *381*, 697.
- (46) Halder, M.; Mukherjee, P.; Bose, S.; Hargrove, M. S.; Song, X.; Petrich, J. W. *J. Chem. Phys.* **2007**, *127*, 055101/1.
- (47) Bose, S.; Adhikary, R.; Mukherjee, P.; Song, X.; Petrich, J. W. *J. Phys. Chem. B* **2009**, *113*, 11061.
- (48) Bose, S.; Adhikary, R.; Barnes, C. A.; Fulton, D. B.; Hargrove, M. S.; Song, X.; Petrich, J. W. *J. Phys. Chem. A* **2011**, *115*, 3630.
- (49) Samanta, A. *J. Phys. Chem. Lett.* **2010**, *1*, 1557.
- (50) Wishart, J. J. *J. Phys. Chem. Lett.* **2010**, *1*, 1629.
- (51) Möller, C.; Plesset, M. S. *Phys. Rev.* **1934**, *46*, 618.
- (52) Hehre, W. J.; Ditchfield, R.; Pople, J. A. *J. Chem. Phys.* **1972**, *56*, 2257.
- (53) Clark, T.; Chandrasekhar, J.; Spitznagel, G. W.; Schleyer, P. v. R. *J. Comput. Chem.* **1983**, *4*, 294.
- (54) Fedorov, D. G.; Olson, R. M.; Kitaura, K.; Gordon, M. S.; Koseki, S. *J. Comput. Chem.* **2004**, *25*, 872.
- (55) Schmidt, M. W.; Baldridge, K. K.; Boatz, J. A.; Elbert, S. T.; Gordon, M. S.; Jensen, J. H.; Koseki, S.; Matsunaga, N.; Nguyen, K. A.; Su, S.; Windus, T. L.; Dupuis, M.; Montgomery, J. A., Jr. *J. Comput. Chem.* **1993**, *14*, 1347.
- (56) Gordon, M. S.; Schmidt, M. W. Advances in electronic structure theory: GAMESS a decade later. In *Theory and Applications of Computational Chemistry: The First Forty Years*; Dykstra, C. E., Frenking, G., Kim, K. S., Scuseria, G. E., Eds.; Elsevier Science: Amsterdam, 2005; p 1167.
- (57) Bode, B. M.; Gordon, M. S. *J. Mol. Graphics Modell.* **1998**, *16*, 133.
- (58) Astleford, B. A.; Goe, G. L.; Keay, J. G.; Scriven, E. F. V. *J. Org. Chem.* **1989**, *54*, 731.
- (59) Drake, G.; Hawkins, T.; Tollison, K. *Energetic Ionic Salts USA*, 2010; Vol. US 7745635.
- (60) Headley, L. S.; Mukherjee, P.; Anderson, J. L.; Ding, R.; Halder, M.; Armstrong, D. W.; Song, X.; Petrich, J. W. *J. Phys. Chem. A* **2006**, *110*, 9549.
- (61) Mukherjee, P.; Crank, J. A.; Halder, M.; Armstrong, D. W.; Petrich, J. W. *J. Phys. Chem. A* **2006**, *110*, 10725.
- (62) Earle, M. J.; Gordon, C. M.; Plechkova, N. V.; Seddon, K. R.; Welton, T. *Anal. Chem.* **2007**, *79*, 758.
- (63) Cross, A. J.; Fleming, G. R. *Biophys. J.* **1984**, *46*, 45.
- (64) Fee, R. S.; Maroncelli, M. *Chem. Phys.* **1994**, *183*, 235.
- (65) Arzhantsev, S.; Ito, N.; Heitz, M.; Maroncelli, M. *Chem. Phys. Lett.* **2003**, *381*, 278.
- (66) Ito, N.; Arzhantsev, S.; Heitz, M.; Maroncelli, M. *J. Phys. Chem. B* **2004**, *108*, 5771.
- (67) Klapötke, T. M. *High Energy Density Materials*; Springer: New York, 2007; Vol. 125.
- (68) Adhikari, A.; Sahu, K.; Dey, S.; Ghosh, S.; Mandal, U.; Bhattacharyya, K. *J. Phys. Chem. B* **2007**, *111*, 12809.
- (69) Mandal, P. K.; Paul, A.; Samanta, A. *J. Photochem. Photobiol. A* **2006**, *182*, 113.
- (70) Khurmi, C.; Berg, M. A. *J. Phys. Chem. Lett.* **2010**, *1*, 161.
- (71) Triolo, A.; Russina, O.; Bleif, H.-J.; Cola, E. D. *J. Phys. Chem. B* **2007**, *111*, 4641.
- (72) Arzhantsev, S.; Hui, J.; Naoki, I.; Maroncelli, M. *Chem. Phys. Lett.* **2006**, *417*, 524.
- (73) Arzhantsev, S.; Jin, H.; Baker, G. A.; Maroncelli, M. *J. Phys. Chem. B* **2007**, *111*, 4978.
- (74) Lang, B.; Angulo, G.; Vauthey, E. *J. Phys. Chem. A* **2006**, *110*, 7028.
- (75) Halder, M.; Headley, L. S.; Mukherjee, P.; Song, X.; Petrich, J. W. *J. Phys. Chem. A* **2006**, *110*, 8623.
- (76) Kobrak, M. N. *J. Chem. Phys.* **2006**, *125*, 064502/1.
- (77) Jin, H.; Baker, G. A.; Arzhantsev, S.; Dong, J.; Maroncelli, M. *J. Phys. Chem. B* **2007**, *111*, 7291.
- (78) Edwards, J. T. *J. Chem. Educ.* **1970**, *47*, 261.
- (79) Bondi, A. *J. Phys. Chem.* **1964**, *68*, 441.
- (80) Tokuda, H.; Hayamizu, K.; Ishii, K.; Susan, M. A. B. H.; Watanabe, M. *J. Phys. Chem. B* **2004**, *108*, 16593.
- (81) Tokuda, H.; Hayamizu, K.; Ishii, K.; Susan, M. A. B. H.; Watanabe, M. *J. Phys. Chem. B* **2005**, *109*, 6103.
- (82) Arzhantsev, S.; Hui, J.; Baker, G. A.; Naoki, I.; Maroncelli, M. Solvation dynamics in ionic liquids, results from ps and fs emission spectroscopy. *Femtochemistry VII*, 2006.
- (83) Dutt, G. B.; Ghanty, T. K. *J. Chem. Phys.* **2002**, *116*, 6687.
- (84) Dutt, G. B. *J. Phys. Chem. B* **2010**, *114*, 8971.
- (85) Horng, M.-L.; Gardecki, J. A.; Maroncelli, M. *J. Phys. Chem. A* **1997**, *101*, 1030.
- (86) Cadena, C.; Maginn, E. J. *J. Phys. Chem. B* **2006**, *110*, 18026.
- (87) Funston, A. M.; Fadeeva, T. A.; Wishart, J. F.; Castner, E. W., Jr. *J. Phys. Chem. B* **2007**, *111*, 4963.